Electronic Supplementary Information (ESI)

High Active (102) Surface Induced Rapid Degradation of CuS Nanotheranostic Platform for in Situ T1-weighted Magnetic Resonance Imaging Guided Synergistic Therapy

Lile Dong,[a,b] Kai Li, [a,b] Ding Wen,[a,b] Yu Lu,[a,c] Kaimin Du,[a,b] Manli Zhang,[a,b] Xuan Gao,[a,b] Jing Feng,[*,a,b] and Hongjie Zhang[*,a,b]

a. State Key Laboratory of Rare Earth Resource Utilization, Changchun Institute of Applied Chemistry, Chinese Academy of Science, Changchun 130022, PR China.

b. University of Science and Technology of China, Hefei 230026, PR China.

c. College of Chemistry, Jilin University, Changchun 130012, P. R. China.

Experimental section

Materials and Characterization: Copper acetylacetonate ($Cu(acac)_2$), oleylamine (OM), sulfur powder (S), and polyvinylpyrrolidone (PVP, $M_W \approx 29000$) were purchased from Sigma-Aldrich. TEM and HR-TEM images and EDS were acquired on a FEI TECNAI G2 microscope. XRD patterns were obtained on a D8 ADVANCE X-ray diffractometer. XPS was obtained on a VG ESCALAB MKII spectrometer. ICP-MS was carried out on an ELAN 9000/DRC. ICP-OES was taken on a PerkinElmer ICP instrument. The *UV–vis–NIR* absorption spectrum was measured by Shimadzu UV-3600 spectrophotometer.

Preparation of CuS NCs: 10 mL of oleylamine containing S (64 mg) were added into 20 mL of chloroform containing copper acetylacetonate (0.5233 g). Then, the mixture was stirred at 70 °C for 20 min. The CuS/OM NCs were isolated by centrifugation and dispersed in dichloromethane (50 mL). Subsequently, 20 mL of dichloromethane containing PVP (4 g) were added into the above solution. The solution was stirred at 70 °C for 4 h. Then, CuS NCs were precipitated and dispersed in PBS.

Cytotoxicity Assessment: CuS NCs were added into the medium and 4T1 murine breast tumor cells (10^4 per well) were incubated at 37 °C and 5% CO_2 for 24 h. Then, MTT (10 μL, 5 mg mL^{-1}) solution was added into each well and the plate was incubated for 4 h at 37 °C and 5% CO_2 in order to form a purple formazan dye. Finally, absorbance of the colored solution at 570 nm was measured by enzyme-linked immunosorbent assay reader. Each experiment was repeated three times.

Reactive Oxygen Species Detection: 4T1 murine breast tumor cells (10^4 cells per well) were treated with CuS NCs and incubated for 6 h. Afterward, the cells were irradiated by 808-nm laser (2 $W \cdot cm^{-2}$, 10 min) and followed by another 16 h of incubation. After that, 20 μL of

ROS-Glo substrate was added to each well and incubated for 2 h. Then, the luminescence intensity of each well was recorded by fluorescence microscope.

Photothermal and Photodynamic Performance in vitro: 4T1 murine breast tumor cells (10^4 cells per well) were treated with CuS NCs and incubated for 6 h. Afterward, the cells were irradiated by 808-nm laser (2 $W \cdot cm^{-2}$, 10 min). The cell viabilities were measured by MTT assays.

Live/Dead Staining Kit: 4T1 murine breast tumor cells (10^4 cells per well) were placed in a 24-well plate and incubated with CuS NCs. Then the tumor cells were irradiated under 808-nm laser with 2 $W \cdot cm^{-2}$ for 10 min. After 18 h incubation, the tumor cells were stained with calcein AM (2 μM) and propidium iodide (PI, 4 μM) for 2 h and observed using fluorescence microscope.

Animal Model: Female kunming mice were obtained from the laboratory animal center of Jilin University (China). The mice were selected for imaging and therapy experiments when their tumors grew to ~100 mm^3. All animal experiments were conducted in strict adherence to the criteria of the regional ethics committee for animal experiments.

***In vitro* and *in vivo* T_1-weighted MRI**: 1.0 mL of physiological or acidic buffer solutions (pH = 7.4 and 6.0) solution containing CuS NCs were measured by 3 T clinical MRI scanner to investigate the effect of T_1-Weighted MRI signal in vitro. Then, we performed T_1-Weighted MRI on tumor-bearing mice by intravenous injection of CuS NCs (200 μL, 16 mg Cu/kg). The parameters are as follows: repetition time = 782 ms, echo time = 20.7 ms, and slice thickness = 2.5 mm.

***In vivo* Photothermal Preformance**: CuS NCs solution (200 μL, 16 mg Cu/kg) was intravenously injected into the tumor-bearing mice. The temperature distribution of the tumor

was monitored and imaged by IR thermal imaging camera at different time intervals (pre, 1, 3, 5 and 10 min) under 808-nm laser irradiation (2 $W \cdot cm^{-2}$, 10 min) after 2 h intravenous injection.

Biodistribution: CuS NCs solution (200 μL, 16 mg Cu/kg) was intravenously injected into the tumor-bearing mice. At 1 h, 2 h, 3 h, 1 d, 4 d and 7 d after administration, the mice were euthanized for analysis of the systemic distribution of CuS NCs (n = 4). After digesting the major organs, tumor, and feces with aqua regia solution for 24 h. The Cu amount per unit mass was quantified by ICP-MS.

In vivo **Photothermal and Photodynamic Synergistic Therapy**: Tumor-bearing mice were randomly allocated into four groups. The mice in the treatment group (CuS+NIR) were intravenously CuS NCs (200 μL, 16 mg Cu/kg)) and irradiated with 808-nm laser irradiation (2 W cm^{-2}, 10 min) at 2 h postinjection. The three control groups including PBS group, NIR group, and CuS group. The tumor volumes of mice were measured by caliper every other day after various treatments and calculated according to the equation $V = L \times W^2/2$ (L and W represent tumor length and tumor width, respectively). Relative tumor volumes were calculated as V/V_0, where V_0 was the tumor volume when the treatment was initiated. Furthermore, the tumor were histological analysis by staining with H&E.

Computational Details: The calculations were carried out using density functional theory (DFT) with the Perdew-Burke-Ernzerbof (PBE) form of generalized gradient approximation functional (GGA).[1] The Vienna ab-initio simulation package (VASP)[2-5] was employed. The plane wave energy cut off was set as 400 eV. The Fermi scheme was employed for electron occupancy with an energy smearing of 0.1 eV. The first Brillouin zone was sampled in the Monkhorst−Pack grid.[6] The 3×3×1 k-point mesh for the calculations. The energy (converged

to 1.0 $\times 10^{-6}$ eV/atom) and force (converged to 0.01eV/Å) were set as the convergence criterion for geometry optimization. The spin polarization was considered in all calculation.

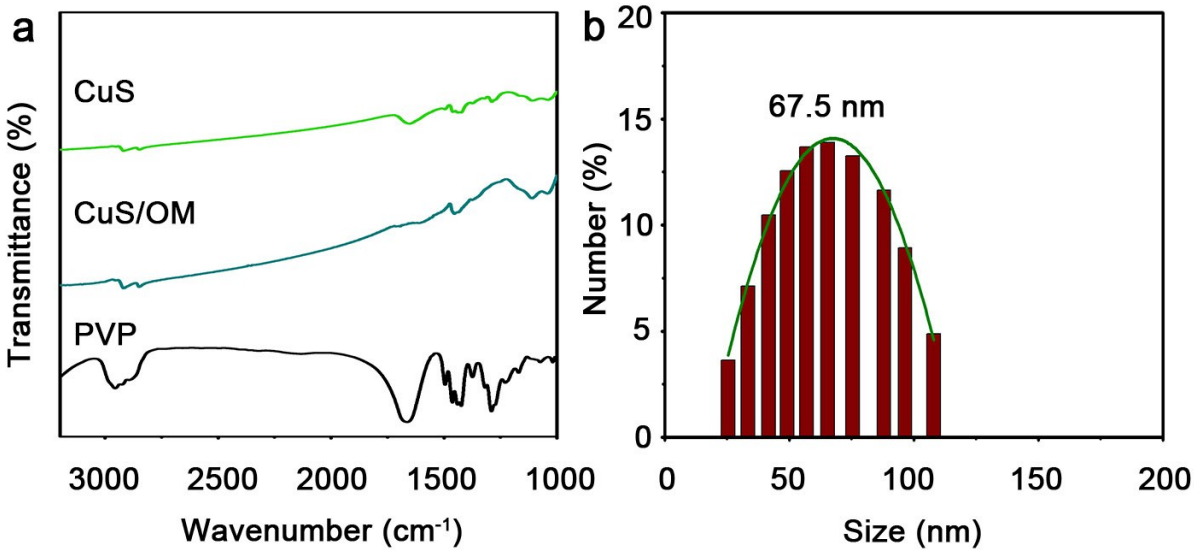

Fig. S1 (a) FTIR spectra of CuS and CuS/OM NCs; (b) Hydrodynamic size distribution of CuS NCs dispersed in water.

The difference between the crystallite size measured by TEM and the hydrodynamic size measured by dynamic light scattering may be attributed to large PVP molecules and water shell. Meanwhile, the zeta potential of CuS NCs physiological (pH = 7.4) buffer solution was about -8 mV.

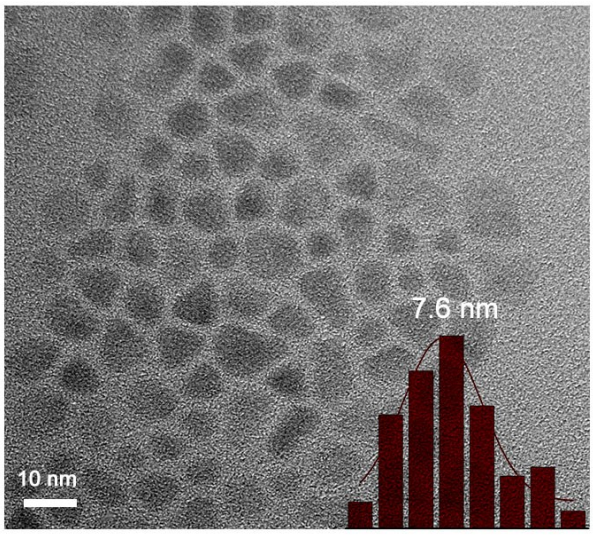

Fig. S2 TEM image and size distribution histograms of CuS/OM NCs.

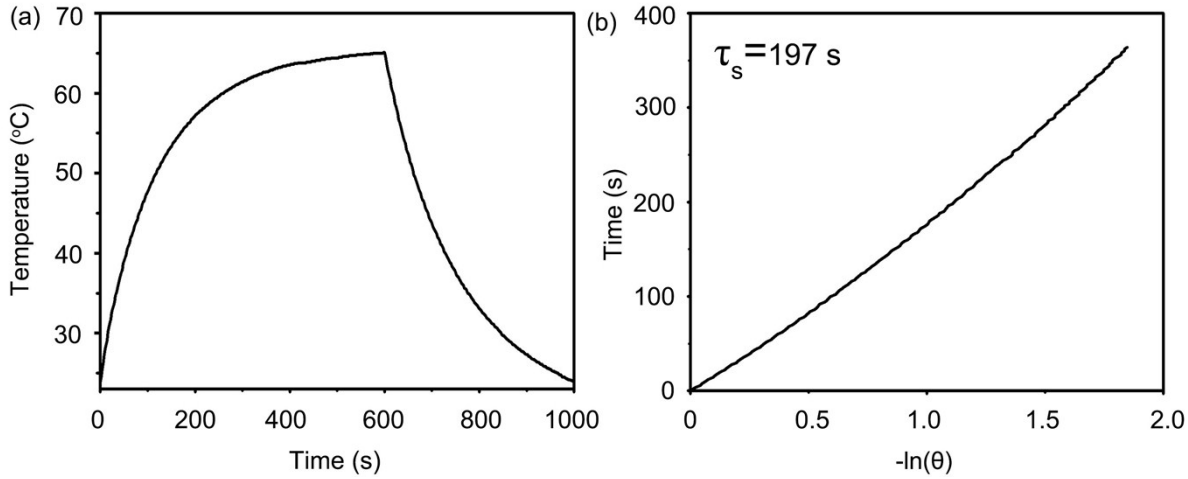

Fig. S3 (a) The temperature elevation profiles of CuS NCs solution upon 808 nm laser irradiation (2 W·cm^{-2}, 10 min) and then the laser was shut off; (b) the corresponding plot of the cooling time versus –ln(θ) obtained from the cooling stage (a).

Table S1 Size (nm), photothermal therapy performances (PTT, η), photodynamic therapy (PDT, Yes or No) performances of various CuS based nanocrystals.

Nanomaterials	Size (nm)	PTT (η)	PDT	References
CuS NCs	7.8	46%	Yes	this work
$Cu_{2-x}S$ NCs	6.5	16.3%	Yes	7
$Cu_{39}S_{28}$ HNPs	40	41.1%	No	8
Cu_9S_5 NCs	70	25.7%	No	9
GSH-CuS NDs	4.8	21.9%	No	10
CSO HMSs	200	48.3%	No	11
Gd:CuS@BSA NPs	9	32.3%	No	12
HCuS@Cu_2S@Au-PRGD	100	35%	No	13
Fe_3O_4@$Cu_{2-x}S$ NPs	8.5	16%	No	14
Fe_3O_4@CuS NPs	120	15.7%	No	15
Cu_3BiS_3 HNSs	80	27.5%	No	16

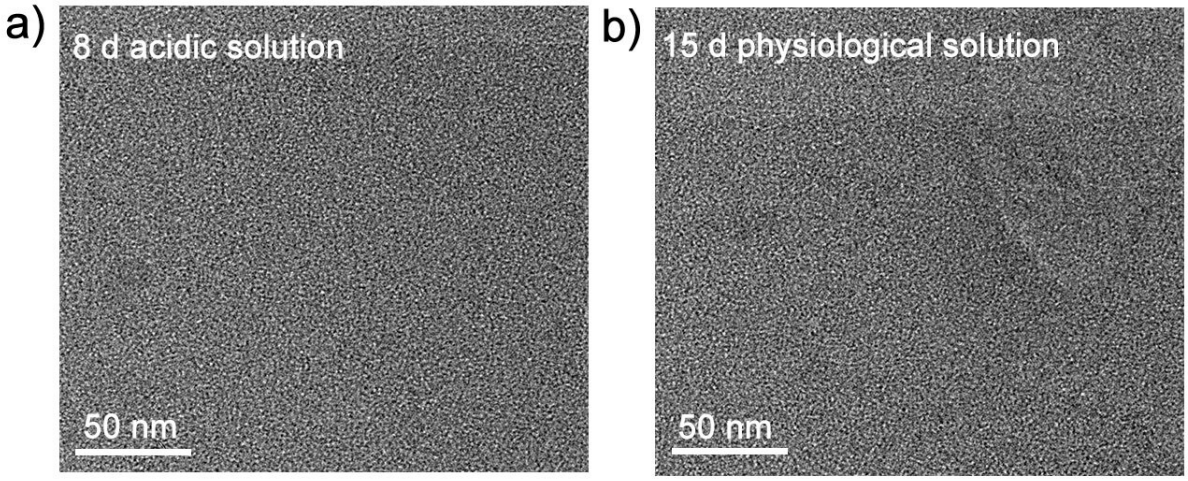

Fig. S4 TEM images of CuS NCs in acidic buffer solutions after 8 d (a) and physiological buffer solutions after 15 d (b).

As displayed in Fig. S4, there were no CuS NCs after 8 days in acidic buffer solutions. Meanwhile, the CuS NCs could not be observed after 15 days in physiological buffer solutions.

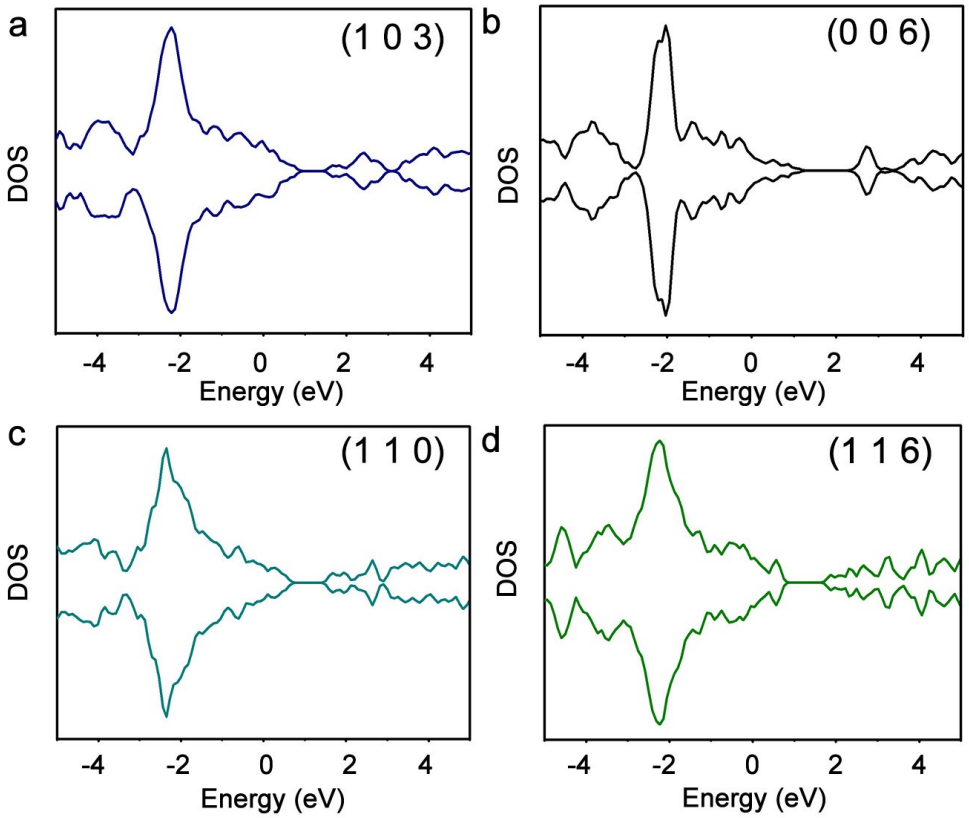

Fig. S5 Density of states of the other main surfaces of CuS NCs.

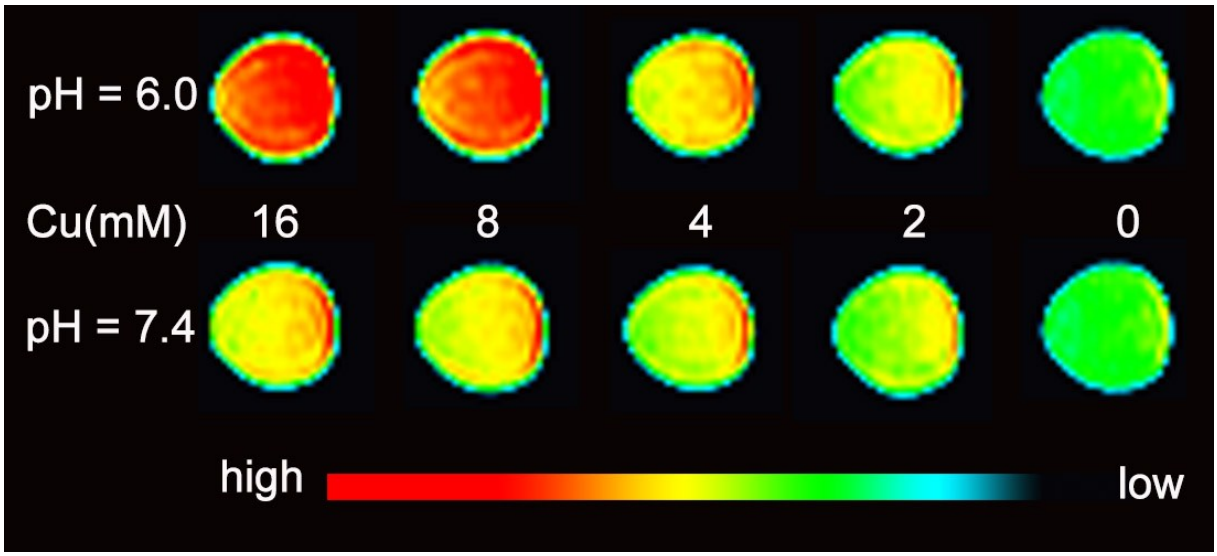

Fig. S6 *In vitro* T_1-weighted MRI of CuS NCs under physiological and acidic buffer solutions (pH = 7.4 and 6.0).

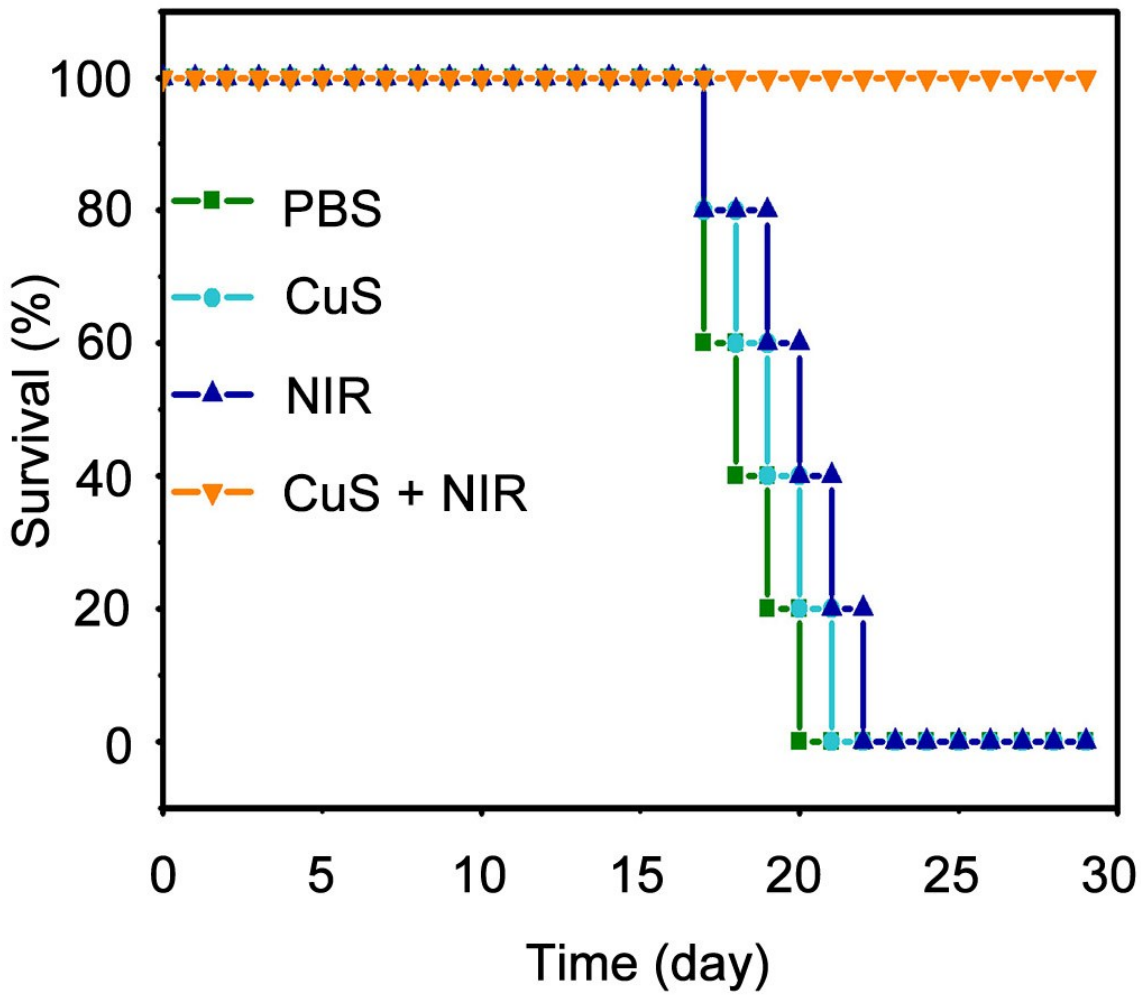

Fig. S7 Survival rates of tumor-bearing mice (n = 10).

References

[1] J. P. Perdew, K. Burke, M. Ernzerhof, *Phys. Rev. Lett.* **1996**, *77*, 3865-3868.

[2] G. Kresse, J. Furthmüller, *Comp. Mater. Sci.* **1996**, *6*, 15-50.

[3] G. Kresse, J. Hafner, *Phys. Rev. B* **1993**, *47*, 558-561.

[4] G. Kresse, J. Hafner, *Phys. Rev. B* **1994**, *49*, 14251-14269.

[5] G.Kresse, J. Furthmüller, *Phys. Rev. B* **1996**, *54*, 11169-11186.

[6] H. J. Monkhorst, J. D. Pack, *Phys. Rev. B* **1976**, *13*, 5188-5192.

[7] S. Wang, A. Riedinger, H. Li, C. Fu, H. Liu, L. Li, T. Liu, L. Tan, M. J. Barthel, G. Pugliese, F. D. Donato, M. S. D'Abbusco, X. Meng, L. Manna, H. Meng, T. Pellegrino, *ACS Nano* **2015**, *9*, 1788-1800.

[8] L. Li, X. Yang, X. Hu, Y. Lu, L. Wang, M. Peng, H. Xia, Q. Yin, Y. Zhang, G. Han, *J. Mater. Chem. B* **2017**, *5*, 6740-6751.

[9] Q. Tian, F. Jiang, R. Zou, Q. Liu, Z. Chen, M. Zhu, S. Yang, J. Wang, J. Wang, J. Hu, *ACS Nano* **2011**, *5*, 9761-9771.

[10] G. Liang, X. Jin, H. Qin, D. Xing, *J. Mater. Chem. B* **2017**, 5, 6366-6375.

[11] Q. Yu, Y. Han, X. Wang, C. Qin, D. Zhai, Z. Yi, J. Chang, Y. Xiao, C. Wu, *ACS Nano* **2018**, *12*, 2695-2707.

[12] W. Yang, W. Guo, W. Le, G. Lv, F. Zhang, L. Shi, X. Wang, J. Wang, S. Wang, J. Chang, B. Zhang, *ACS Nano* **2016**, *10*, 10245-10257.

[13] X. Deng, K. Li, X. Cai, B. Liu, Y. Wei, K. Deng, Z. Xie, Z. Wu, P. Ma, Z. Hou, Z. Cheng, J. Lin, *Adv. Mater.* **2017**, *29*, 1701266.

[14] Q. Tian, J. Hu, Y. Zhu, R. Zou, Z. Chen, S. Yang, R. Li, Q. Su, Y. Han, X. Liu, *J. Am. Chem. Soc.* **2013**, *135*, 8571-8577.

[15] Z. Wu, W. Li, C. Luo, C. Su, C. Yeh, *Adv. Funct. Mater.* **2015**, *25*, 6527-6537.

[16] Zhou, D. Ma, S. Zhang, W. Wang, W. Chen, S. Huang, K. Yu, *Nanoscale*, **2016**, *8*, 1374-1382.